Green Chemistry

Two-zone ligand-assisted displacement chromatography for producing high-purity praseodymium, neodymium, and dysprosium with high yield and high productivity from crude mixtures derived from waste magnets

SCHOLARONE™
Manuscripts

Two-zone ligand-assisted displacement chromatography for producing high-purity praseodymium, neodymium, and dysprosium with high yield and high productivity from crude mixtures derived from waste magnets

Yi Ding, David Harvey, and Nien-Hwa Linda Wang*

Davidson School of Chemical Engineering, Purdue University, 480 Stadium Mall Drive, West Lafayette, IN, 47907-2100, United States.

*Corresponding author: wangn@purdue.edu

Abstract

Three rare earth elements (REEs), neodymium (Nd), praseodymium (Pr), and dysprosium (Dy), are essential ingredients of permanent magnets, used widely in electronics, motors, hybrid cars, generators, televisions, sensors, and windmills. Conventional methods for producing high-purity REEs employ two-phase liquid-liquid extraction methods, which require thousands of mixer-settler units in series or in parallel and generate large amounts of toxic wastes. In this study, a two-zone ligand-assisted displacement chromatography (LAD) system with a new zone-splitting method is developed for producing high-purity (>99%) Nd, Pr, and Dy with high yields (>99%) and high sorbent productivity from crude REE mixtures derived from waste magnets. The zone-splitting method based on selectivity-weighted composition factors enables a two-zone design to achieve two orders of magnitude higher productivity than that of a single column design. The design and simulation methods are based on first principles and intrinsic (or scale-independent) engineering parameters. They can be used to design processes for a wide range of feed compositions or production scales. The overall productivity of the two-zone LAD can exceed 100 kg REEs/m^3/day, which is 100 times higher than those of the conventional extraction methods. The LAD for the purification of the ternary mixture requires only three chromatography columns, a safe extractant, EDTA, and other environmentally friendly chemicals. Most of the chemicals can be recycled, generating little waste. This method has the potential for efficient and environmentally friendly purification of the REEs from waste magnets. The method may also help transform the current linear REE economy (from ores to pure REEs, to products, to landfills) to a circular and sustainable REEs economy.

1. Introduction

Rare earth elements (REEs) include the 15 elements in the lanthanide series plus scandium (Sc) and yttrium (Y). They are essential ingredients for magnets, metal alloys, polishing powders, catalysts, ceramics, and phosphors, which are important for high-technology and clean energy applications (Fig. 1).[1–6] Although the total market value of REEs is only $1.5 billion, the market value of the products that require REEs exceeds $5 trillion.[7]

About 30 wt.% of rare earth elements are used to produce NdFeB permanent magnets,[5] which are widely used in hard drive disks, wind turbine generators, and electric vehicle motors. Three key REEs in NdFeB magnets are Nd, Dy, and Pr. The first two are classified as critical materials by the U.S. Department of Energy, which aims at generating 20% of the electricity from wind energy by 2030.[6] Each direct-drive permanent generator for 1 MW of electricity will require between 160 to 650 kg of permanent magnets made from Nd, Pr, and Dy.[6] Such generators are increasingly used in offshore and large onshore installations because of their high energy efficiency.[6,8] Rare earth permanent magnets are also used in the motors of the hybrid and electric vehicles. It is estimated that each hybrid or electric vehicle requires 1.5 to 2.5 kg of REE-based permanent magnets.[9]

The market of the key REEs in magnets is highly volatile because their production is concentrated in a few regions around the world. China now controls over 80% of the world REEs supplies and more than 95% of the supplies of rare earth alloys and magnets.[7] This control could lead to manufacturing of over 90% of the high-tech products in China by 2040.[7] The REE production in other regions is limited by a lack of technical expertise in production, high capital costs, and the significant environmental impacts of the conventional methods.[10,11]

Production of REEs starts from the beneficiation and concentration of REE ores such as bastnäsite, a rare earth fluorocarbonate salt containing about 7-8% of rare earth oxide (REO) equivalent. After crushing and grinding, chemical steam conditioning, flotation, and cleaning, bastnäsite can be upgraded to a concentrated REE crude that contains about 60% REO. The REE crude is further digested, purified, and refined to pure metals.[1,12]

The REE purification process is the most difficult step because the REEs present in the crude have similar physical and chemical properties.[13] Current industrial purification procedures still use liquid-liquid extraction methods developed in the 1950s. Such methods require thousands of mixer-settler units to produce high-purity REEs. It is difficult to adapt the liquid-liquid extraction methods to different feedstocks or production scales. These methods are energetically and chemically intensive, requiring the use of toxic extractants, organic solvents, concentrated acids for stripping, and generating large amounts of acidic and toxic wastes. To produce one ton of rare earth oxides, about 30 tons of wastewater are released into the environment.[14] The extraction processes also consume large amounts of ammonia for the saponification of the organophosphorus extractant, as well as a large volume of hydrochloric acid for stripping of the extractant. On average only 35% of the ammonia used in the process is recovered as ammonium chloride.[15] Life cycle analysis studies reveal that in the production of REEs from bastnäsite, the purification steps in the conventional processes account for about 1/3 of the total environmental impact in terms of global warming, carcinogen and non-carcinogen human toxicity, eutrophication, and ecotoxicity. Furthermore, they contribute 70% of the ozone depletion impact in the production process.[14,15]

Recycling waste magnets can be a potential method for producing valuable REEs materials. About 300,000 tons of REEs are present in permanent magnets produced to date, and about 3,300 to 6,600 tons of REEs can be recovered per year from waste magnets.[4] As solid-state disks (SSD) start to

dominate the market, many HDDs containing REEs are projected to be available for recycling. Purified REEs derived from waste magnets can be reused in other energy and defense applications.

Recycling REEs from waste streams, such as waste magnets, can reduce the environmental risks associated with mining. Producing heavy rare earth oxides from clays containing adsorbed REE ions can cause underground water contamination and severe vegetation and topsoil removal. Large amounts of mine tailings and wastewater discharge into the environment may lead to permanent damage to ecosystems, loss of biodiversity, and human health issues. [16]

The recovery of REEs from waste magnets is potentially profitable based on the Sherwood analysis (Fig. 2), which gives an order of magnitude predictions of the price, or the production cost, as a function of the concentration of the target product in the feedstock. In general, the higher the concentration, the lower the production cost, and hence the market price. In Fig. 2, a Sherwood correlation line was obtained by fitting the prices of 10 metals and their weight fractions in mineral ores. Estimated feedstock cost[17] and purification costs of Nd, Pr, and Dy from waste magnets are summarized in Table 1. The Sherwood analysis shows that waste magnets are promising feedstocks for producing Dy, Nd, and Pr, with a potential profit about $5/kg waste magnets.

Various methods have been developed for recovering crude REE mixtures from waste magnets. The most commonly used method is oxidation of the metals into metal oxides, followed by selective acid leaching.[18–23] The waste magnets were ground into fine particles and oxidized at elevated temperatures. Then the metal oxides were dissolved in acids. Other metal oxides (Fe, Ni, Co, B) were also removed via selective leaching or precipitation,[19,24] membrane-assisted solvent extraction,[23] or ionic liquid extraction.[20,25] The REEs in the waste magnets can also be converted to soluble chloride salts by various methods, including roasting with ammonium chloride under inert atmosphere,[26] chlorination using chlorine gas,[27] or selective extraction using magnesium and

potassium chlorides molten salts.[28] Other methods have also been tested for converting REEs in waste magnets into hydroxides, including hydrothermal treatment[29] and hydrolysis after vacuum induction melting.[30] With most of the recovery methods in the literature, more than 90% of the REEs in the waste magnets can be extracted as mixtures of REE chlorides or hydroxides with little contamination of the other elements in the waste magnets.

Separating the crude REE mixtures derived from waste magnets into pure individual REEs is critical for producing metal alloys or other applications. Solvent extraction using an organophosphoric extractant in an ionic liquid was tested previously.[22,31,32] However, only two REEs (Nd and Dy) were recovered with high purity, and the liquid-liquid extraction methods are inefficient for REE purification because the interfacial areas per unit processing volume for mass transfer are two to three orders of magnitude lower than those in adsorption or chromatography. A functionalized silica adsorbent was tested for separating Dy from other REEs derived from waste magnets, but the adsorbent was costly and had limited stabilities, and the Dy purity was low (~70%).[33]

Since conventional low-cost adsorbents or ion exchangers have insufficient selectivities for REE purification, a chelating agent (or a ligand) in the mobile phase can be used to substantially increase the selectivity. The feasibility of ligand-assisted displacement chromatography for REE purification was first reported in the 1950s.[34–36] Nonetheless, since no process simulations or systematic design methods were available, the literature LAD separation processes were designed empirically. Some experiments for separation of three REEs took several months.[35] Hence, it is infeasible to use empirical methods for developing efficient LADs for large scale separation of REEs.

It was known that if the column length is sufficiently long, a constant-pattern displacement train can form in non-ideal LAD systems (i.e. systems with diffusion or dispersion effects).[37] However, no general theory was available for predicting the formation of a constant pattern in LAD until 2018. Choi et al. developed a general correlation to enable designs of LAD systems with the minimum column lengths to reach constant-pattern states, in which high purity bands with sharp boundaries form as a result of displacement effects.[37] Operating at constant-pattern states can help achieve high purity products with high yields and high sorbent productivities. A constant-pattern design method was developed for non-ideal systems based on the general correlation and an equation for the yield of the target component.[38] The yield is a function of several key dimensionless groups, which control the constant-pattern mass transfer zone length. The design method was tested and verified using simulations and experiments for different target yields, ligand concentrations, and feed compositions. The productivities achieved using this design method for a single column were over 800 times higher than literature results for ternary separations with the same purity and similar yields.[38]

The general correlation of Choi et al. was derived from rate model simulations based on the constant separation factor (CSF) isotherm model, which is applicable to REE feed mixtures containing a ligand. If an REE feed mixture contains no ligand, the feed REEs will not separate in the loading zone, since most adsorbents have negligible selectivities for different REEs. The REE separation will occur only after a ligand is introduced after loading. For such cases, the loading zones are shorter, and higher loading velocities can be used to shorten the loading times. An improved isotherm model and simulations are presented in this study to simulate the separation processes more closely for REE crudes with no ligand, and a revised general correlation for the conditions required for reaching the constant-pattern state has been developed.

The studies of Choi et al. were focused on the separation of equimolar ternary REE mixtures. However, the REE concentrations in the feedstock derived from waste magnets differ by one order of magnitude (Table 1). Achieving high yields of high-purity Dy (the minority component) in a single column requires an extremely narrow mass transfer zones between the two adjacent elution bands, and a small linear velocity for fixed selectivities and mass transfer coefficients. The overall elution time is long because of the small linear velocity, resulting in a low productivity. Hence, a design involving more than one column, or one zone, is developed in this study. An efficient splitting strategy is developed for the separation of complex feed mixtures to obtain high-purity REEs with high yields and high productivities.

Therefore, the specific objectives of this study are the following:

(1) Develop and test experimentally an improved constant-pattern design method for ligand-assisted displacement chromatography for feed mixtures containing no ligand initially.

(2) Develop a new zone-splitting strategy and a two-zone LAD method for achieving high-purity, high-yield and high-productivity separations of ternary mixtures that have minority components.

(3) Use simulations and experiments to test the two-zone purification method for the purification of three REEs (Nd, Pr, and Dy) from a synthetic mixture with a similar composition to typical REE crudes derived from waste magnets.

In this study, we introduced new simulations, which have higher accuracy in simulating the LAD loading process for REE crude mixtures with no ligand. Most of the crude mixtures derived from waste magnets or other sources contain no ligand. The most important contribution of this work is the new splitting strategy for separating complex crude REEs mixtures with a wide range of

concentrations. The new two-zone LAD method can achieve more than 100 times higher sorbent productivity than the single column method of Choi et al. This new splitting strategy is a major theoretical breakthrough for the separation of complex mixtures. The results of this study have the potential to transform current REEs separation and purification processes into green and clean processes, provide a driving force for producing high-purity REEs from waste magnets, and help achieve a circular REE economy (Fig. 3).

2. Theory

2.1 Constant-pattern isotachic train and the general constant-pattern correlation

Ligand-assisted displacement chromatography uses a ligand (chelating agent) in the mobile phase to separate REEs into pure components. Details for the separation mechanism are given in the Supplementary Information Section S1. The formation of an isotachic (constant speed) train in a long column is a distinct feature of displacement chromatography. In an ideal system, all components will form rectangular solute bands and migrate at the same velocity. In a non-ideal system, the boundaries between adjacent solute bands (or concentration waves) are spread because of diffusion or dispersion effects. The overlapping regions decreases as the bands begin to separate because they migrate at different velocities (Fig. 4). Eventually, wave spreading due to diffusion or dispersion effects is counterbalanced by wave sharpening due to displacement effects, in which the concentration waves reach a "constant pattern" and each mass transfer zone length reaches a fixed value, $L_{MTZ,CP}$.[37]

In this study, a new general correlation (Eq. (1)) was developed using the modulated Langmuir isotherm (see S2), which can simulate the LAD process more closely for REE crudes containing

no ligand. The detailed derivation of the mass transfer zone length and the development of the new general correlation, Eq. (1), can be found in S2.

$$\phi_{min} = 1 + 1.5e^{-\frac{X}{9.8}} \#(1)$$

ϕ_{min} is the minimum column length to reach a constant-pattern isotachic train for a non-ideal system divided by that for an ideal system, X is the product of the loading fraction L_f, the dimensionless overall mass transfer coefficient k_f^*, and a selectivity term $(\frac{\alpha^e - 1}{\alpha^e + 1})$. The general correlation divides the two-dimensional space into two regions: a constant-pattern region and a transient-pattern region (Fig. 5). One can use this "map" to predict whether the concentration waves between the two adjacent bands can reach constant pattern for the given system and operation parameters. Furthermore, this general correlation, Eq. (1), has been incorporated into the constant-pattern design method for the separation of feedstocks with no ligand. The details are given in S3.

2.2. Trade-off curve between yield and productivity for a complex mixture with a minority component

If a single column is used for producing a product with a desired purity, there is a trade-off between yield and productivity. To increase the yield of a target component, a slow mobile phase velocity is required to sharpen the waves and reduce the lengths of the overlapping regions with the adjacent bands. However, the slow velocity results in a small sorbent productivity. If a high velocity is used to increase sorbent productivity, the waves are more spread and the lengths of the overlapping regions increase, resulting in a lower yield. This relation between yield and productivity is known as the "trade-off" curve for a single column.

If the goal is to use a single column to recover only one REE with a target yield, the design results for an REE mixture with mole fractions of 0.83 for Nd, 0.12 for Pr, and 0.05 for Dy are shown in Fig. 6. The curves were generated based on the constant-pattern designs with a fixed breakthrough cut θ of 0.05.[37] In practice, breakthrough curves can be monitored using online detectors. A design with a fixed breakthrough cut is easy to implement for collecting products. However, to satisfy the component mass balance requirement at a constant-pattern state, only two out of the three variables (purity, yield, and breakthrough cut, θ) can be specified in the design for a single column, see S4. For a fixed θ of 0.05, the resulting yield, productivity, and product purity for recovering a single REE (Dy, Pr, or Nd) from the REE mixture are shown in Fig. 6. The purity for the target component exceeds 99% if the target yield is greater than 63.5%. The curves are "approximate" trade-off curves, since the target product purities are not fixed, and they vary slightly from 99% to over 99.9%.

If a single column is designed to recover the minority component Dy with a high purity (99.9%) and a high yield of 95%, a very slow velocity is required to sharpen the concentration waves to minimize the mass transfer zone lengths (the overlapping regions of two adjacent bands), resulting in a very low sorbent productivity, 0.04 kg Dy/m³/day, Fig. 6. In contrast, for producing the majority component Nd with the same purity and yield from the same feedstock, the productivity is 64.2 kg Nd/m³/day, which is 1,600 times higher than that of Dy. If the target yield of Nd is lowered from 95% to ca. 77%, the productivity of Nd can be further increased to 120 kg Nd/m³/day while the purity of Nd is 99.5%. The results in Fig. 6 show that for producing a high-purity product (>99%) from the complex feedstock, the sorbent productivity highly depends on the target component.

Generally, if a single column is used for the recovery of a single component from a complex mixture, the product purity is controlled by the breakthrough cut θ and the yield of the target component. The sorbent productivity is controlled by a selectivity-weighted composition factor γ_i, defined in Eq. (2).[38]

$$\gamma_i = \frac{x_i}{\dfrac{\alpha_{i,i-1}^e + 1}{\alpha_{i,i-1}^e - 1} + \dfrac{\alpha_{i+1,i}^e + 1}{\alpha_{i+1,i}^e - 1}} \#(2)$$

The yield Y_i and the sorbent productivity $P_{R,i}$ are related to the γ_i values by Eq. (3) and Eq. (4):[38]

$$Y_i = 1 - \frac{\beta}{2\gamma_i L_f k_f^*} \#(3)$$

$$P_{R,i} = \frac{\varepsilon_b c_d u_0 x_i L_f}{L_c}\left(1 - \frac{\beta}{2\gamma_i L_f k_f^*}\right)\#(4)$$

where x_i is the mole fraction of component i in the feed mixture; β is the natural logarithm of the ratio of $(1 - \theta)$ to θ, where θ is the breakthrough cut; $\alpha_{i,i-1}^e$ is the selectivity between component i and the component eluting ahead of component i; $\alpha_{i+1,i}^e$ is the selectivity between the component eluting after component i and component i; ε_b is the bed void fraction; c_d is the effective ligand concentration, u_0 is the linear interstitial velocity of the mobile phase; and L_c is the column length,

For an equimolar mixture, where x_i is the same for all components, the component i with the highest selectivities will have the narrowest mixed band regions between its two adjacent bands (See S2, Eq.(S2)). This component will have the highest value of γ_i, the highest yield, and the highest productivity.

For a complex mixture, if the selectivity between each pair of the adjacent components was the same, the constant-pattern mass transfer zone length would be the same for all solute bands (See

S2, Eq. (S2)). As x_i increases, the displacement band becomes wider. The component with the highest mole fraction has the highest yield, because the overlapping region relative to total displacement band width is the smallest, and the yield loss due to the mixed band relative to total amount is the smallest. The component with the largest x_i value or the largest γ_i value has the highest yield and the highest productivity.

Therefore, the selectivity-weighted composition factors γ_i account for the effects of composition and selectivity. The component with the largest γ_i value can be separated from a mixture with the highest productivity using a single column. The γ_i values for the ternary mixture are listed in Table 2. In this mixture, Dy has the smallest γ_i value, hence it is separated from the mixture with the smallest productivity, whereas Nd, which has the largest γ_i value, is separated from the mixture with the largest productivity, Fig. 6.

If a single column is used to recover all three components with high yields and high purities from the mixture, the velocity or flow rate is limited by the yield requirement for Dy, the component with the smallest γ_i value. If the design aims to recover Dy with 95% yield, the productivities of Nd and Pr are also small because of the low velocity. As a result, the total REE productivity is only 0.7 kg/m^3/day (Fig. 6).

However, if the separation of the three REEs occurs in two separate zones, one can recover high-purity REEs with high yield and high productivity. A systematic splitting strategy is developed. The component with the largest γ_i value, Nd, is recovered first with a high purity and high productivity in Zone I. The two mixed bands of Zone I, Dy/Nd and Nd/Pr, are then sent to Zone II for further separation. The mixed band material in Zone II is then recycled to the inlet of Zone II to achieve high yields (99%) for all three components. In this method, the productivity and the

yield of each component are no longer limited by the trade-off curves for a single column. The overall productivity of a two-zone design with high purity (>99.5%) and high yield (>99%) for all three REEs is more than 100 times higher than that of the single column design with similar product purity and 95% yield of Dy, Fig. 6. The two-zone design is explained in more detail in the next section.

2.3 Constant-pattern design of a two-zone LAD for the separation of a ternary REE mixture of Dy, Nd, and Pr

The constant-pattern design method for a single column reported previously[38] was modified in this study by incorporating the new general correlation, Eq. (1), and the new zone-splitting strategy based on the γ_i values of Eq. (2). An overview of this design method is shown in Fig. 7. The multi-zone, constant-pattern design method is based on the advanced wave theories, general zone splitting strategies, and the intrinsic (or scale-independent) parameters. This method applies to many production scales and can handle complex feed mixtures with multiple components and widely different concentrations. For desired product purities and yields, if the intrinsic parameters, the feed composition, and volume are known, the method can generate the zone configuration, column size, and the optimal operating velocity for each zone to achieve the maximum sorbent productivity. The design and the optimization algorithm are explained in detail in S4.

For the separation of a ternary mixture of Dy (5%), Nd (83%), and Pr (12%), a schematic of the design is shown in Fig. 8. Zone I is designed to recover the majority of Nd, which has the highest γ_i value in the original feed. In Zone I, Step 1, the column is pre-equilibrated with Cu^{2+} solution. In Step 2 the feed mixture is fed into a Cu^{2+}-loaded column. In Steps 3-7, a ligand solution (EDTA-Na) is loaded into the column, separating the feed mixture into three fractions: a Dy/Nd mixed band, a pure Nd band (the target product of Zone I), and a Nd/Pr mixed band. After all the REEs

are eluted from the column, the column is in the Na$^+$ form and then pre-saturated again using Cu^{2+} solution. The Dy/Nd mixed band from Step 5 and the Nd/Pr mixed band from Step 7 are sent to Column II-A and Column II-B in Zone II, respectively. The mixed bands from the Zone II columns are collected and recycled directly back to Columns II-A and II-B to further increase the yields. For simplicity, the recycle streams within Zone II and the column washing steps are not shown in Fig. 8.

Rate model simulations were developed for Zones I and II using the software VERSE,[37–39] which was developed at Purdue. Batch LAD experiments were done first to test the rate models based on the modulated multicomponent Langmuir isotherm and the intrinsic parameters. The verified isotherm and parameters were used to design a two-zone LAD system for the separation of a ternary mixture with a similar REE composition as in waste magnets.

3. Materials, Apparatus, and Procedures

3.1. Materials

Neodymium(III) nitrate hexahydrate (Nd(NO$_3$)$_3$·6H$_2$O, 99.9% REO), dysprosium (III) nitrate pentahydrate (Dy(NO$_3$)$_3$·5H$_2$O, 99.9% REO), and copper chloride dihydrate (CuCl$_2$·2H$_2$O, >99%) were purchased from Alfa Aesar. Praseodymium(III) nitrate hexahydrate (Pr(NO$_3$)$_3$·6H$_2$O, 99.9%) and blue dextran were purchased from Sigma-Aldrich. Ethylenediamine tetraacetic acid (EDTA) disodium salt dihydrate (C$_{10}$H$_{14}$N$_2$Na$_2$O$_8$·2H$_2$O, crystalline), sodium hydroxide (NaOH), and hydrochloric acid (HCl) (36.5%~38%) were purchased from Fisher Chemical. Ultrapure deionized water (DI) was produced with a Milli-Q purification system.

3.2. Column packing

The cation exchange resin AG-MP 50 (100-200 mesh) was purchased from Bio-Rad Laboratories. Two Vantage® L chromatography laboratory columns were purchased from Millipore. A slurry packing method was used to pack the column.[38] The final packed bed lengths were 38 cm and 89 cm, respectively.

3.3. Chromatography column tests

The chromatography experiments were performed using an AKTA Explorer 100 system. The effluent from the column was monitored online using an Agilent 1260 infinity photodiode array (PDA) detector. The effluent was collected in fractions using an Agilent 440-LC fraction collector.

3.4. Inductively coupled plasma optical emission spectroscopy (ICP-OES) analysis

The elemental analysis was done using a Thermo iCAP 7400 inductively coupled plasma optical emission spectrometer. The mixed rare earth ICP standard (50 ppm) was purchased from Sigma-Aldrich. Trace metal grade nitric acid (HNO_3) for sample preparation was purchased from Fisher Chemicals. The samples were diluted and prepared using metal-free centrifuge tubes purchased from VWR.

3.5. Preparation of EDTA ligand solutions

The ligand solution was prepared by dissolving EDTA disodium salts in DI water and using sodium hydroxide solution to adjust pH to the desired value. The pH of the ligand solution was 9, and the nominal EDTA concentration was 0.09 M. The pH values of the solution were measured using a Mettler-Toledo S220 Seven Compact pH meter.

3.6. Verification of the general map

The improved general map was tested experimentally using equimolar Nd and Pr binary mixtures. The column tests were run in the 38-cm column. The experimental conditions are summarized in

Table S2 in Section S5. The column effluent was monitored using an Agilent PDA detector. Wavelengths of 700 nm, 575 nm, and 444 nm were chosen to monitor the Cu, Nd, and Pr, respectively.

3.7. Testing of Zone I

Two packed columns were connected with a total column length of 127 cm. The ternary mixture which mimics REEs crude derived from waste magnets was prepared and separated using LAD. Since the focus of this study is to test the improved constant-pattern design method and the new splitting strategy, a synthetic mixture instead of an actual waste crude mixture was used in the LAD tests in order to have a better control of the feedstock composition. The detailed experimental conditions and simulation parameters are summarized in Table S3. In Zone I, the feed concentrations were 0.05 N Dy, 0.83 N Nd, and 0.12 N Pr.

The column effluent was monitored with an Agilent PDA detector. The effluent was also collected in fractions using the Agilent 440-LC fraction collector. The Dy concentrations were analyzed with ICP-OES.

3.8. Testing of Zone II

In Zone I two mixed bands were generated, one with Cu/Dy/Nd and one with Nd/Pr. More than 10 runs of Zone I were needed to generate enough mixed band materials to test the separation in Zone II. The effluent history for the separation of the mixed bands in Zone II was examined using synthetic mixtures. The concentrations of REEs in the mixed bands were calculated from the elution profile from Zone I. Note that the REEs mixed bands collected from LAD tests were mixtures of EDTA-REEs complexes rather than aqueous solutions of free REE ions.

For preparing a mixed band of Cu/Dy/Nd, 3.143 g $Dy(NO_3)_3 \cdot 5H_2O$ and 3.872 g $Nd(NO_3)_3 \cdot 6H_2O$ were dissolved in DI water first. The mixture was loaded into a copper-loaded column. The REEs were stripped off from the column using 0.09 M EDTA at pH=9. The mixed band was collected before a concentration decrease in Cu was observed, and the loaded REEs were collected in the mixed band. When this mixed band was diluted to 500 ml, the final concentrations of Dy and Nd were 0.043 N and 0.053 N. The experimental conditions and simulation parameters for the separation of Dy and Nd are summarized in S5, Table S4. The effluent was monitored using a PDA detector and collected in fractions for measuring Dy concentrations using ICP analysis.

To prepare a mixed band of Nd/Pr, 2.513 g $Nd(NO_3)_3 \cdot 6H_2O$ and 2.146 g $Pr(NO_3)_3 \cdot 6H_2O$ were dissolved in 0.09 M EDTA solution (pH=9). About 1.04 g NaOH was added into the solution to prevent EDTA precipitation at low pH. The final solution volume was 200 ml, and the concentration of Nd and Pr were 0.086 N and 0.074 N, respectively. The conditions for the separation of Nd and Pr are summarized in S5, Table S5.

4. Experimental Results and Discussion

4.1. Tests of the rate model simulations

The rate model simulation results were compared with literature data,[40] where erbium (Er) was used as the presaturant and EDTA was used as the ligand. The simulation parameters are summarized in Table S6. The sorbent was a cation exchange resin AG 50X12 with sulfonic functional groups. The simulation results are in good agreement with the experimental data, indicating the accuracy of the rate model simulations and the model parameters (Fig. 9). In Moore's work, Er, instead of Cu, was used as the presaturant. The selectivity between REEs in the

feed and Er was 1.1 during the loading and increased to 1.95 after the ligand was introduced into the column.

The rate model simulations and the general map were compared with separation data (Fig. 10). A binary mixture (0.3 N Nd, 0.3 N Pr) was prepared and fed into a 38-cm column. The Nd/Pr selectivity was 1.8, as measured previously.[37] The mass transfer coefficients were estimated in our previous study.[38] By changing the loading volume, different loading fractions (L_f) and dimensionless column lengths (ϕ) were obtained. The X values corresponding to the ϕ values were calculated from the general correlation. The dimensionless mass transfer coefficients (k_f^*) were calculated from the X values, and the flow rates were obtained from the k_f^* values. Five different feed volumes and their corresponding flow rates were used. The measured mass transfer zone lengths matched closely with the constant-pattern mass transfer zone lengths from the simulations and those from the general correlations (Fig. 10).

4.2. Design and testing of Zone I

The improved general correlation was used for designing a ternary separation system using a synthetic mixture with a similar composition as a REE crude derived from waste magnets (0.05 N Dy, 0.83 N Nd, 0.12 N Pr) (Fig. 11a). The actual effective selectivity between Dy and Nd should be quite high because of a large difference between the ligand affinities. The Dy/Nd selectivity in the design was set as 5, which is sufficient to produce sharp waves in the design and the simulations.

The pH of the REE feed solutions in our experiments was 4, which is typical for REE crudes derived from waste magnets. (For actual waste materials, after acid dissolution of the waste magnets, the solution pH was adjusted to 4 to precipitate the Fe(III) ions, which is a typical impurity.[22]) For the REE crude solution at pH 4, the small amounts of H^+ ions in the feed did not

affect the loading or the subsequent separation of REEs in LAD. The pH of the ligand (EDTA) solution was important, because it could affect the ligand binding efficiency for REEs. The distribution of the various EDTA species in solution depends on the initial pH of the solution. At high pH (>12), EDTA can lose four protons from its carboxylic acid groups, the number of which affects the EDTA binding efficiency with REEs. At a constant EDTA concentration, the higher the solution pH, the more carboxylate groups are "free" to bind with REEs, and the higher the eluted REE band concentrations. The initial pH of the EDTA solution, however, could not be higher than 11, because REE ions could precipitate at such a high pH.

The design for Zone I aimed to maximize the productivity of Nd in a single column. The yield for the highest Nd productivity was predicted to be 77.5%. The detailed experimental conditions are listed in Table S3. The pH of the ligand solution was kept at 9. The experimental elution profiles were compared with simulations in Fig. 11. The design target yield for Nd in Zone I and the experimental yield and productivity of Nd for each test are summarized in Table 3. The target yields agree to within 1% with the experimental yields. The productivity of Nd exceeded 100 kg/m^3/day in Zone I.

4.3. Design and testing of Zone II

To further increase the yield of Nd and to collect high purity Dy and Pr, the mixed bands of Dy/Nd and Nd/Pr (shaded grey regions in the elution profile) in Zone I could be collected and further separated in Zone II. Simulants with similar concentrations were run for demonstrating the Zone II separation.

In Zone I, an aqueous solution containing REE ions was fed directly to the column. The mixed bands collected from Zone I were then fed into Zone II. In Zone I, the REE ions were adsorbed together with no separation and formed a uniform mixture band near the column inlet, since

selectivity was negligible. REE ions started separating after the EDTA ligand solution was introduced into the column. In the theoretical model and simulations, the selectivity change was accounted for by the modulated Langmuir isotherm, as explained in S2.

The REE ions in the feed of Zone II were bound to EDTA, and the apparent displacement occurred during the feed loading. The REEs start separating during the loading because EDTA has different selectivities for the different REEs. The REE loading region was wider in Zone II than in Zone I, because EDTA is bound to the REEs during their migration. It was important to confine the REEs in a short fraction of the column length during the loading, in order to leave sufficient column length for further separation after the loading is finished. For this reason, a safety factor of 100% extra column length was incorporated in the Zone II design. Although such a large safety factor was used to demonstrate the separation in Zone II, in practice the actual safety factor can be smaller. The same design algorithm was used for both columns used in Zone II. The column length in the design program was 50% of the actual column length in the experiments, 89 cm.

The elution profiles are shown in Figs. 11b and 11c, and the experimental yields and productivities are summarized in Table 3. The detailed experimental and simulation parameters are given in the Experimental section and S4. In Zone II Column A, the Nd yield target in the design was 73.4% to maximize the productivity, and the experimental yield of Nd was 89%. In the experiments, the mixed band between Nd and Na bands was defined as "pure" Nd, because in practice it is easy to separate Nd from Na by precipitating Nd as an oxalate or carbonate. In Zone II Column B, the Nd yield target was 74.6%, and the experimental yield was 74%. Recycling the mixed bands (Fig. 11) from the two columns in Zone II back to the feed of Zone II can further increase the yields of all components to 99% or higher.

4.4. Theoretical predictions of the REE yields in a Two-Zone LAD

The established theoretical model and the rate model simulations for both Zones I and II are in good agreement with the data in Sections 4.2 and 4.3. The experimental yields match closely or exceed the design target yields, with all components having a purity over 99%. The key condition for achieving a 99% yield for each component is the recycling and re-feeding the mixed bands in Zone II. Because experimental demonstrations of recycling mixed bands in Zone II can be tedious, VERSE simulations of LAD processes were done instead. The column length was 100 cm in the design and 120 cm in the simulations for a 20% safety factor. The Dy/Nd mixed band from a single run of Zone I was used as the feed for Zone II Column A, and the Nd/Pr mixed band from Zone I was the feed for Zone II Column B.

For Zone II Column A, the two mixed bands, Cu/Dy and Dy/Nd, were collected and mixed with the original feed for Column A. The new mixture was used as the feed for Zone II Column A in Run 2. The loading volume and the flow rate remained the same. The feed of Zone II Column A in Run 3 contained the Cu/Dy and Dy/Nd bands collected from Run 2 mixed with the original feed. In Run 3, the column outputs, the yields, and the component purities remained the same as in Run 2. The results indicated that the system reached a cyclic steady state after Run 3 (Table 4). A similar process was implemented in Zone II Column B for the separation of the Nd/Pr mixed band. The system also reached a cyclic steady state after Run 3. By continuously recycling the mixed bands in the two-zone LAD, little REE in the mixture was lost. The overall yields for all components were over 99%.

The overall yields and productivities for the three components are summarized in Table 5 and compared to those for the single column design with a fixed breakthrough cut. To achieve an overall REE yield of 99% and a purity of greater than 99.5% for each component using a similar

column length (~1.2 m), the productivity of the single column process is more than two orders of

magnitude smaller than that in the two-zone LAD process (Fig. 6).

4.5. Comparisons between LAD and conventional liquid-liquid extraction

The most widely used REE separation technology in industry is multi-stage liquid-liquid

extraction.[42] In this process, an organophosphorus extractant dissolved in kerosene is used for

extracting REEs from the aqueous phase. Concentrated HCl solutions (up to 6 M) are needed for

stripping off REEs from the extractant, and a concentrated ammonia solution is used as a

saponification agent. Large fractions of the acid and base used are not recoverable, leading to large

amounts of acidic wastewater containing a high concentration of ammonia salts.[14,42] Moreover,

kerosene is flammable, and organophosphorus extractants are toxic.

By contrast, since only environmentally benign chemicals are used in LAD, the safety of the

process is much improved, and the environmental impact is much lower. The LAD process

generates sodium salt byproducts, which can be converted electrochemically into base and acid.[43]

The EDTA-Cu complexes eluting from the column can be easily recovered as EDTA and copper

salts. The recovery yields of EDTA and Cu are quite high (>95%).[44] High purity REEs can be

precipitated from EDTA-REE complexes using oxalate salts, and the ligand can be recovered with

high yields and can be reused. Hence, little waste is generated.

The design of two-zone LAD is based on advanced theories and the intrinsic adsorption and mass

transfer parameters. This method can be easily scaled up to any production scale, and the operating

conditions can be easily adapted for REE crude mixtures with a wide range of compositions. Most

of the chemicals in LAD can be recovered and reused. By contrast, in conventional liquid-liquid

extraction methods most of the acids and bases are consumed during the purification process and

cannot be economically recycled. For this reason, the chemical costs of LAD are much lower. The

extraction methods would require hundreds to thousands of mixer-settler units for producing the three REEs with high purities (99.5%) and high yields (>99%). LAD requires only three chromatography columns with 100 times smaller volume, resulting in a much lower capital cost. Overall, LAD is much more efficient, economical and environmentally friendly than the liquid extraction method for producing high-purity REEs. Table 6 summarizes the advantages of LAD over the extraction process.

5. Conclusions

Rare earth elements are essential for high-technology products. Conventional mining and separation processes for producing high-purity REEs can have large environmental impacts. Recycling REEs from a waste stream such as waste magnets is technically feasible and potentially profitable, and it would reduce the need for mining processes. In this study, an environmentally benign separation method, two-zone ligand-assisted displacement chromatography, has been developed for producing high purity REEs with high yields and high productivities.

An improved model based on modulated Langmuir isotherms has been developed and used to simulate the ligand-assisted displacement chromatography accurately for REE feedstocks with no ligand. A general correlation for such feeds was developed for predicting the minimum column length for the formation of a constant-pattern displacement train. A design method based on the correlation was developed. The rate model and the simulations were tested and verified for the literature data for the separation of seven REEs. Moreover, the general correlation was tested and verified with new experimental data for the separation of binary mixtures of Nd and Pr.

A precise zone splitting strategy based on the selectivity-weighted composition factors γ_i was developed and tested for two-zone LAD for the separation of a complex mixture of Dy, Nd, and

Pr. In the first zone, high purity Nd was obtained with a yield of 78% and a productivity higher than 100 kg/m³/day. A second zone was designed to separate the mixed bands from the first zone to produce all three REEs with high purity and high yield. The overall Nd yield was 95% without recycling the mixed bands in Zone II. Recycling the Nd/Pr and Dy/Nd mixed bands of Zone II can increase the overall yields further to more than 99% for all three REEs. For similar product purity and yield, the overall productivity for this two-zone LAD system was 111 kg REE/(m³ sorbent)/day, more than 100 times higher than that of the single column LAD.

The two-zone LAD requires only a few columns and the productivity is about 100 times higher than the average volume productivity of the conventional liquid-liquid extraction, which requires thousands of mixer-settler units. The LAD separation process uses only environmentally friendly chemicals, most of which can be recycled and reused, generating little waste. The multi-zone LAD method has the potential to transform the REE purification process into a cleaner and "greener" process. The results of this study may also help change the current linear REE economy (from ores to pure REEs, to products, to landfills) to a circular and sustainable REE economy.

Nomenclature

Variables	Definition
α^e	Effective sorbent selectivity
$\alpha_{ij}^{sorbent}$	Sorbent selectivity between component i and j
α_{ij}^{ligand}	Ligand selectivity between component i and j
γ_i	Selectivity weighted composition factor
ε_b	Bed void fraction
ε_p	Particle porosity
θ	Breakthrough cut [35, 36]
ϕ	Dimensionless column length relative to the minimum column length required to form an isotachic train in an ideal system
c_d	Effective ligand concentration (N)
C_f	Feed concentration (N)
$D_{b,i}$	Brownian diffusivity of component i (cm^2/min)
$D_{p,i}$	Pore diffusivity of component i (cm^2/min)
ID	Column internal diameter (cm)
k_f^*	Dimensionless overall mass transfer coefficient
L_C	Column length (cm)
L_f	Loading fraction
L_{MTZ}	Mass transfer zone length (cm)
$L_{MTZ, CP}$	Constant-pattern mass transfer zone length (cm)
ΔP_{max}	Maximum pressure drop
q_{max}	Effective sorbent capacity (eq./L)
u_0	Linear velocity (cm/min)
V_f	Feed loading volume (mL)
x_i	Molar fraction of component i
X	Product of L_f, k_f^*, and $\frac{\alpha^e - 1}{\alpha^e + 1}$

Table 1 Feedstock costs, processing costs, and potential profits of producing Dy, Nd, and Pr from waste magnets

	Weight Percent (%)	Estimated Production Cost ($/kg REE)	Feedstock Costs ($/kg REE)	Market Price ($/kg REE)
Nd	27	1	19	52
Pr	4.0	6	2.8	93
Dy	1.5	15	0.2	298
REEs Revenue ($/kg feedstock)	Average Production Cost ($/kg feedstock)	Feedstock Costs ($/kg feedstock)	Profit ($/kg feed)
22.2	6 ± 2	11*	**5**

* The cost of waste magnets was estimated to be $11/kg waste magnets (including the cost for dismantling from HDDs and the magnets collecting cost).[17]

Table 2. Concentration and selectivity of REEs in a mixture derived from waste magnets

Component	Molar fraction (x_i)	$\alpha^e_{i,i-1}$	$\alpha^e_{i+1,i}$	$\gamma_i = \dfrac{x_i}{\dfrac{\alpha^e_{i,i-1}+1}{\alpha^e_{i,i-1}-1} + \dfrac{\alpha^e_{i+1,i}+1}{\alpha^e_{i+1,i}-1}}$
Dy	0.05	>>1	5	0.020
Nd	0.83	5	1.8	0.166
Pr	0.12	1.8	>>1	0.027

Table 3. Yields and productivities of Nd in Zone I and Zone II

	Zone I	Zone II Column A	Zone II Column B
Target yield (%)	77.5	73.4	74.6
Experimental yield (%)	78	89	74
Experimental purity (%)	99.3	99.8	99.5
Productivity (kg/m^3/day)	133.0	88.0	14.4

Table 4. The simulation results for recycling mixed bands in Zone II.

	Run 1			Run 2			Run 3		
	Feed concentration (N)	Yield (%)	Purity (%)	Feed concentration (N)	Yield (%)	Purity (%)	Feed concentration (N)	Yield (%)	Purity (%)
	Zone II Column A								
Dy	0.043	69.9	99.2	0.048	77.1	99.4	0.048	77.1	99.4
Nd	0.053	87.5	99.8	0.051	89.3	99.8	0.051	89.3	99.8
	Zone II Column B								
Nd	0.086	76.7	99.3	0.087	79.7	99.5	0.087	79.7	99.5
Pr	0.074	81.3	99.6	0.072	81.3	99.6	0.072	81.3	99.6

Table 5. The comparison between the two-zone design and the single column design.

Element	Two-Zone design			Single-Zone design		
	Yield (%)	Purity (%)	Average Productivity (kg/m^3/day)	Yield (%)	Purity (%)	Average Productivity (kg/m^3/day)
Dy	>99	99.4	6.3	95.3	99.9	0.04
Nd	>99	99.5	92.2	99.5	99.9	0.59
Pr	>99	99.6	12.0	96.7	99.9	0.08
Overall	>99	-	111.5	99	-	0.7

Table 6. Comparison between liquid-liquid extraction and two-zone LAD

	Liquid-liquid extraction	Two-Zone LAD	Advantages of LAD
Typical yield, %	80-95	>99	No loss of REEs
Scalability	Difficult to adapt to various feed and scale	Model-based design enables easy adaptability to any feed and scale	More versatile
Normalized productivity	1	100	Much more efficient
Normalized processing volume	100	1	Much smaller
Extractant	Toxic organophosphorus compounds	EDTA	Safer
Solvents	Flammable organic solvents (kerosene) and water	Water	Safer and cleaner
Other Chemicals	High concentration acid (up to 6 M) for stripping and ammonia for saponification	Dilute acid, dilute base, Cu^{2+} solution (can be recycled)	Environmentally friendly
Waste	50 tons wastewater per ton REO produced with 2.6 tons ammonium salts, pH=0.9	Little	Much less waste

Acknowledgements

Conflicts of interest

There are no conflicts to declare.

References

1   C. K. Gupta and N. Krishnamurthy, *Extractive Metallurgy of Rare Earths*, 2005.

2   J. Navarro and F. Zhao, *Front. Energy Res.*, 2014, **2**, 1–17.

3   M. Humphries, *Rare earth elements: The global supply chain*, 2012.

4   K. Binnemans, P. T. Jones, B. Blanpain, T. Van Gerven, Y. Yang, A. Walton and M. Buchert, *J. Clean. Prod.*, 2013, **51**, 1–22.

5   N. A. Mancheri, B. Sprecher, G. Bailey, J. Ge and A. Tukker, *Resour. Conserv. Recycl.*, 2019, **142**, 101–112.

6   D. D. Imholte, R. T. Nguyen, A. Vedantam, M. Brown, A. Iyer, B. J. Smith, J. W. Collins, C. G. Anderson and B. O'Kelley, *Energy Policy*, 2018, **113**, 294–305.

7   D. S. Abraham, *The Elements of Power: Gadgets, Guns, and the Struggle for a Sustainable Future in the Rare Metal Age*, Yale University Press, 2015.

8   S. Hoenderdaal, L. Tercero Espinoza, F. Marscheider-Weidemann and W. Graus, *Energy*, 2013, **49**, 344–355.

9   T. Elwert, D. Goldmann, F. Roemer and S. Schwarz, *J. Sustain. Metall.*, 2017, **3**, 108–121.

10   N. K. Foley, A. Ayusor, C. R. Bern, B. E. Hubbard and J. A. Vazquez, *Acta Geol. Sin. - English Ed.*, 2014, **88**, 428–430.

11   S. Massari and M. Ruberti, *Resour. Policy*, 2013, **38**, 36–43.

12   British Geological Survey, *Rare Earth Elements*, 2010.

13   L. Ling and N. H. L. Wang, *J. Chromatogr. A*, 2015, **1389**, 28–38.

14   E. Vahidi and F. Zhao, *J. Environ. Manage.*, 2017, **203**, 255–263.

15   J. C. K. Lee and Z. Wen, *J. Ind. Ecol.*, 2017, **21**, 1277–1290.

16   X. J. Yang, A. Lin, X.-L. Li, Y. Wu, W. Zhou and Z. Chen, *Environ. Dev.*, 2013, **8**, 131–136.

17   H. Jin, B. D. Song, Y. Yih and J. W. Sutherland, *J. Clean. Prod.*, 2019, **211**, 257–269.

18   T. Itakura, R. Sasai and H. Itoh, *J. Alloys Compd.*, 2006, **408–412**, 1382–1385.

19   H. M. Dhammika Bandara, K. D. Field and M. H. Emmert, *Green Chem.*, , DOI:10.1039/c5gc01255d.

20   J. Kitagawa and R. Uemura, *Sci. Rep.*, 2017, **7**, 8039.

21   A. Kumari, M. K. Sinha, S. Pramanik and S. K. Sahu, *Waste Manag.*, 2018, **75**, 486–498.

22   S. Riaño and K. Binnemans, *Green Chem.*, 2015, **17**, 2931–2942.

23   D. Kim, L. E. Powell, L. H. Delmau, E. S. Peterson, J. Herchenroeder and R. R. Bhave, *Environ. Sci. Technol*, 2015, **49**, 22.

24   T. Vander Hoogerstraete, B. Blanpain, T. Van Gerven and K. Binnemans, *RSC Adv.*, 2014, **4**, 64099–64111.

25   T. Vander Hoogerstraete, S. Wellens, K. Verachtert and K. Binnemans, *Green Chem.*, 2013, 919–927.

26   M. Itoh, K. Miura and K. Machida, *J. Alloys Compd.*, 2009, **477**, 484–487.

27   Y. Mochizuki, N. Tsubouchi and K. Sugawara, *ACS Sustain. Chem. Eng.*, 2013, **1**, 655–

662.

28   Z. Hua, J. Wang, L. Wang, Z. Zhao, X. Li, Y. Xiao and Y. Yang, *ACS Sustain. Chem. Eng.*, 2014, **4**, 2536–2543.

29   N. Maat, V. Nachbaur, R. Larde, J. Juraszek and J.-M. Le Breton, *ACS Sustain. Chem. Eng.*, 2016, **4**, 6455–6462.

30   Y. Bian, S. Guo, L. Jiang, J. Liu, K. Tang and W. Ding, *ACS Sustain. Chem. Eng.*, 2016, **4**, 810–818.

31   Y. Dong, X. Sun, Y. Wang, C. Huang and Z. Zhao, *ACS Sustain. Chem. Eng.*, 2016, **4**, 1573–1580.

32   K. Wang, H. Adidharma, M. Radosz, P. Wan, X. Xu, C. K. Russell, H. Tian, M. Fan and J. Yu, *Green Chem.*, 2017, 19, 4469–4493.

33   X. Zheng, E. Liu, F. Zhang, Y. Yan and J. Pan, *Green Chem.*, 2016, **18**, 5031–5040.

34   F. H. Spedding, E. I. Fulmer, J. E. Powell and T. A. Butler, *J. Am. Chem. Soc.*, 1950, **72**, 2354–2361.

35   F. H. Spedding, J. E. Powell and E. J. Wheelwright, *J. Am. Chem. Soc.*, 1954, **76**, 2557–2560.

36   R. E. Lindstrom, *Separation of rare-earth elements in bastnasite by ion exchange*, 1959.

37   H. Choi, D. Harvey, Y. Ding and N. L. Wang, *J. Chromatogr. A*, 2018, **1563**, 47–61.

38   H. Choi, D. Harvey, Y. Ding and N.-H. L. Wang, *J. Chromatogr. A*, 2018, **1580**, 49–62.

39   J. A. Berninger, R. D. Whitley, X. Zhang and N. H. L. Wang, *Comput. Chem. Eng.*, 1991, **15**, 749–768.

40   B. W. Moore, L. J. Froisland and A. E. Petersen, *Rapid Separation of Heavy Rare-Earth Elements*, 1995.

41   W. Maketon, C. Z. Zenner and K. L. Ogden, *Environ. Sci. Technol.*, 2008, **42**, 2124–2129.

42   D. Qi, *Hydrometallurgy of Rare Earths*, Elsevier, 2018.

43   *US Pat.* 8,936,770 B2, 2015.

44   *US Pat.* 3,138,637, 1964.

45   F. Xie, T. A. Zhang, D. Dreisinger and F. Doyle, *Miner. Eng.*, 2014, **56**, 10–28.

46   S. Yin, K. Chen, C. Srinivasakannan, S. Li, J. Zhou, J. Peng and L. Zhang, *Hydrometallurgy*, 2018, **175**, 266–272.
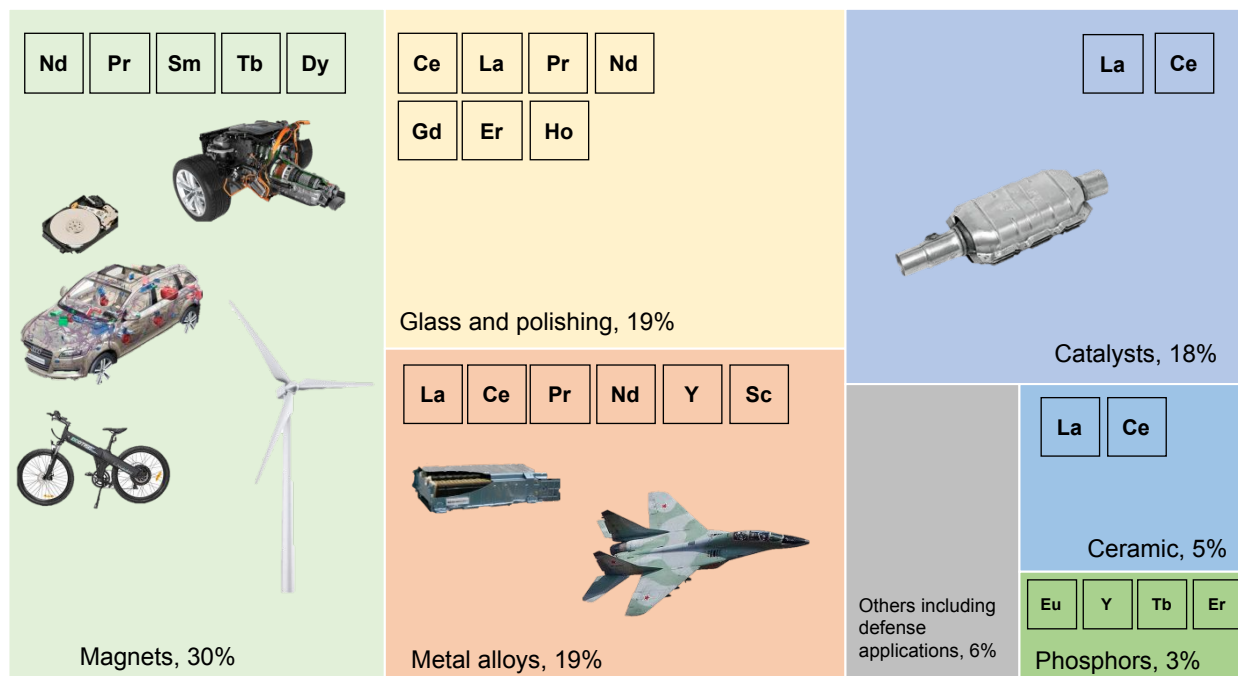
Figure 1. Breakdown of REEs (by weight) in different applications.
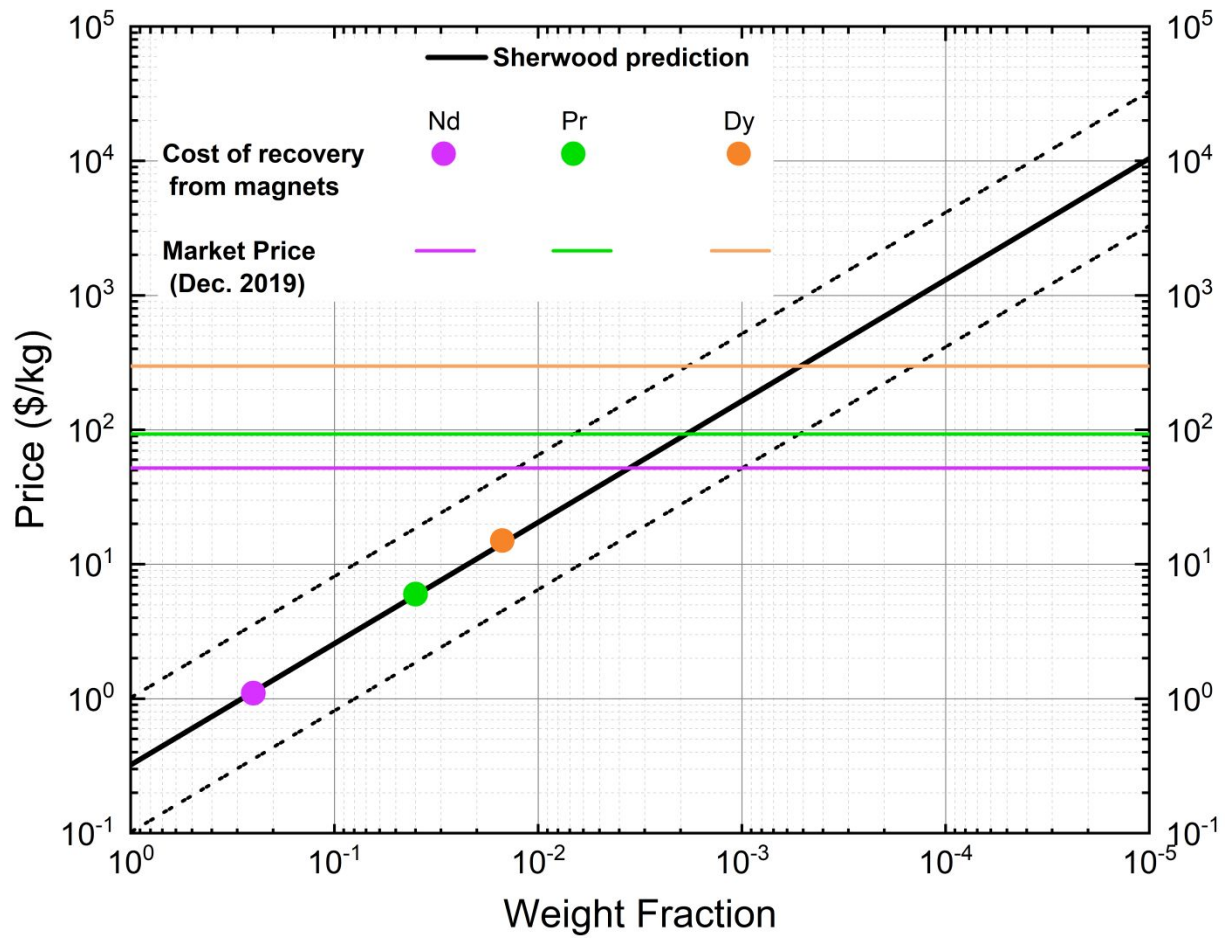
Figure 2. Sherwood prediction on process costs for purifying REEs from magnets.
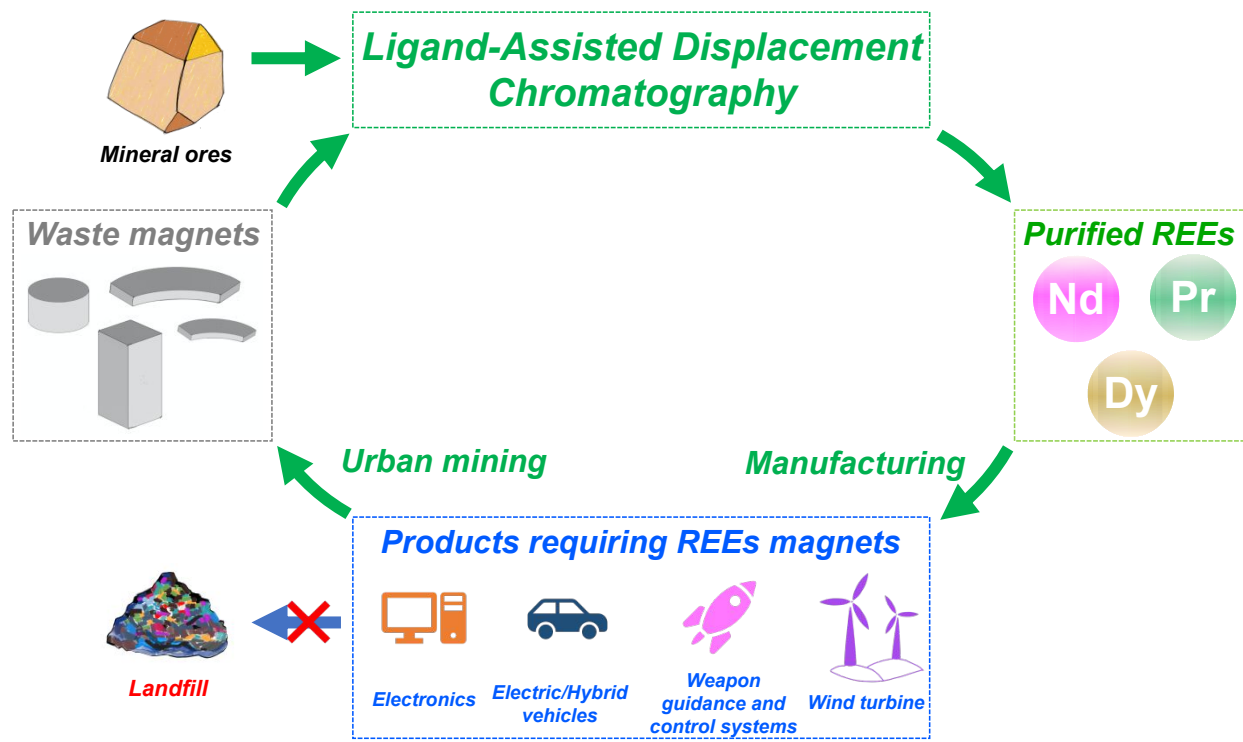
Figure 3. Circular economy of REEs supply chain.
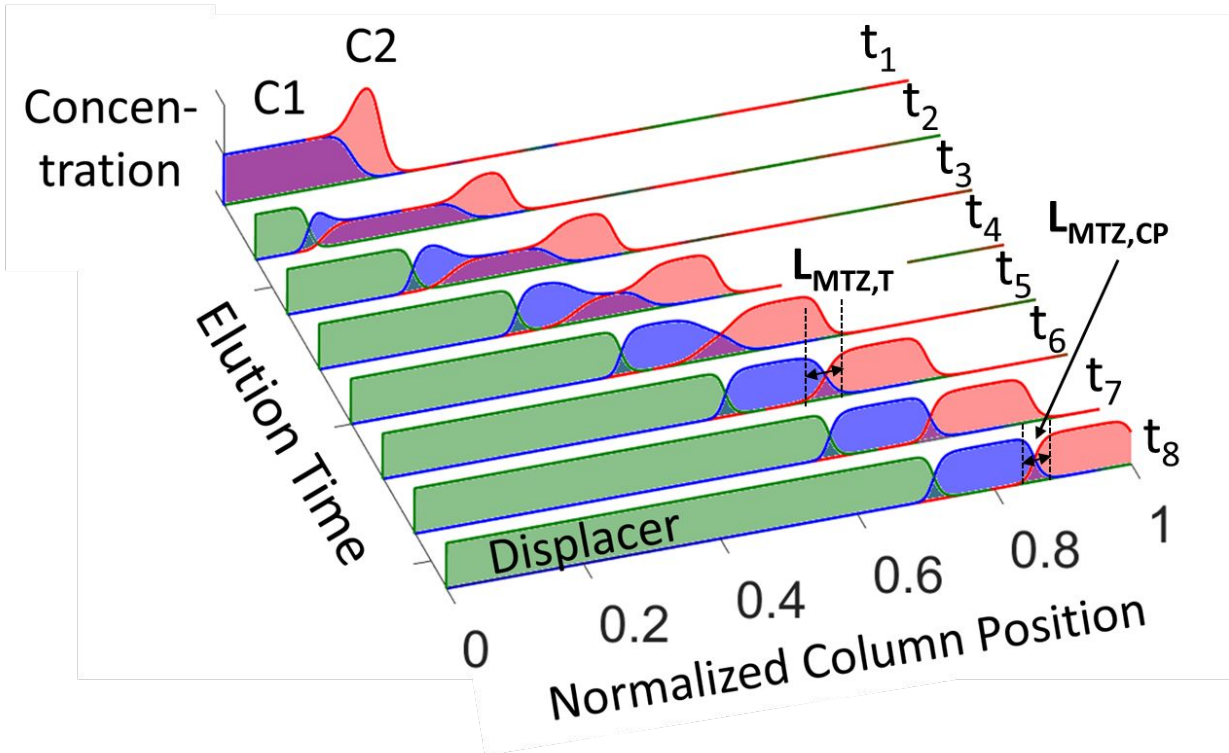
Figure 4. Development of a constant pattern isotachic train in a non-ideal LAD system. The "pink" REE, which has a higher affinity for the ligand, migrates at a higher speed than the "blue" REE, which has a lower affinity for the ligand. Eventually, at the constant-pattern state t8, two separated bands form and migrate at the same speed, while the band shape and the length of the mass transfer zone ($L_{MTZ,CP}$) remain fixed during migration.

$$X = L_f k_f^* \frac{\alpha^e - 1}{\alpha^e + 1}$$
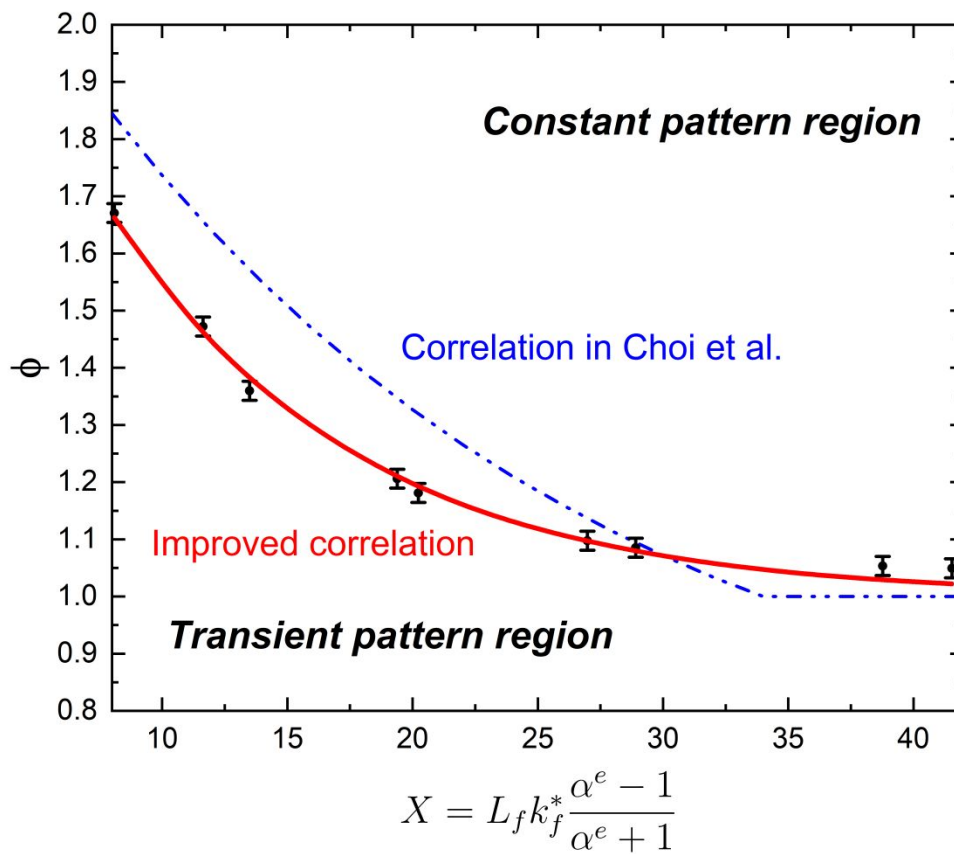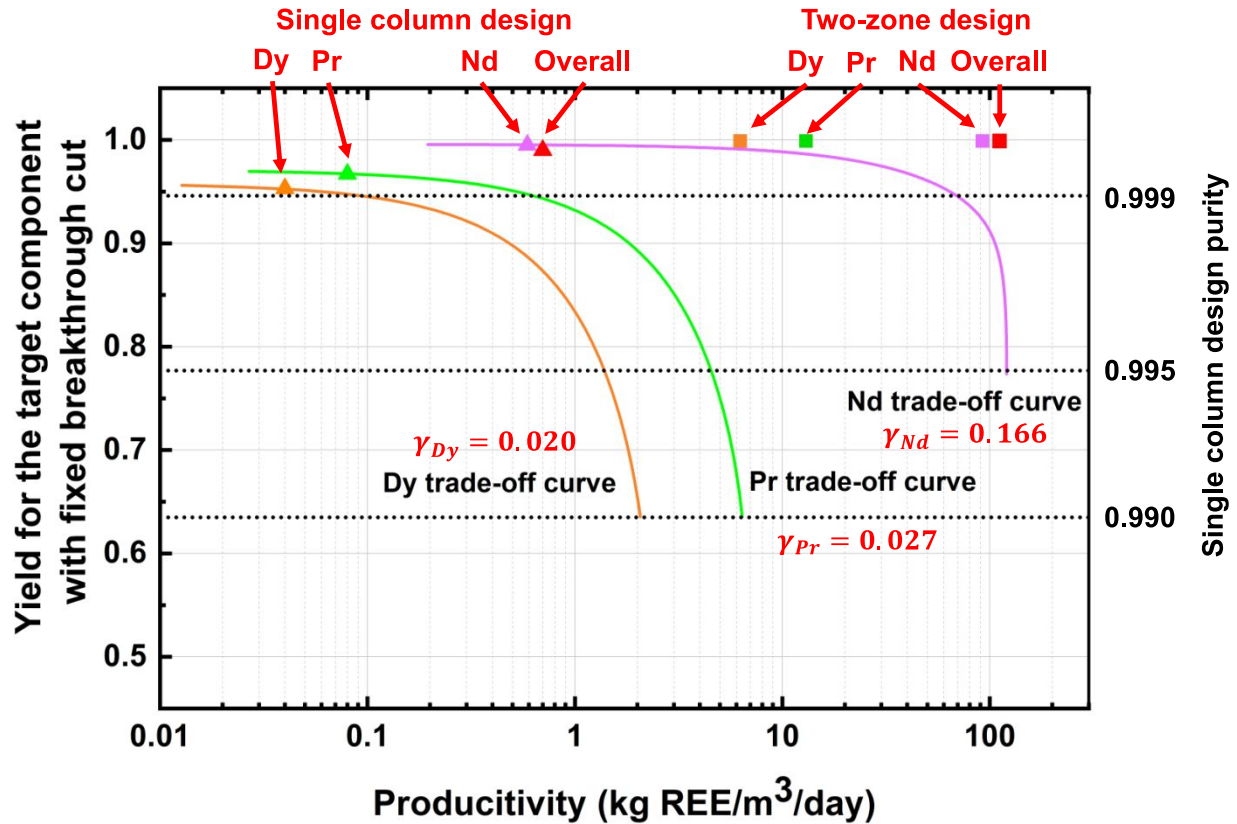
Figure 5. The constant-pattern general map.

Figure 6. Theoretical trade-off curves between yield and productivity for a constant-pattern LAD deign for producing 99% pure products from the chosen ternary complex REE mixture using a single column with a fixed breakthrough cut ($\theta = 0.05$).
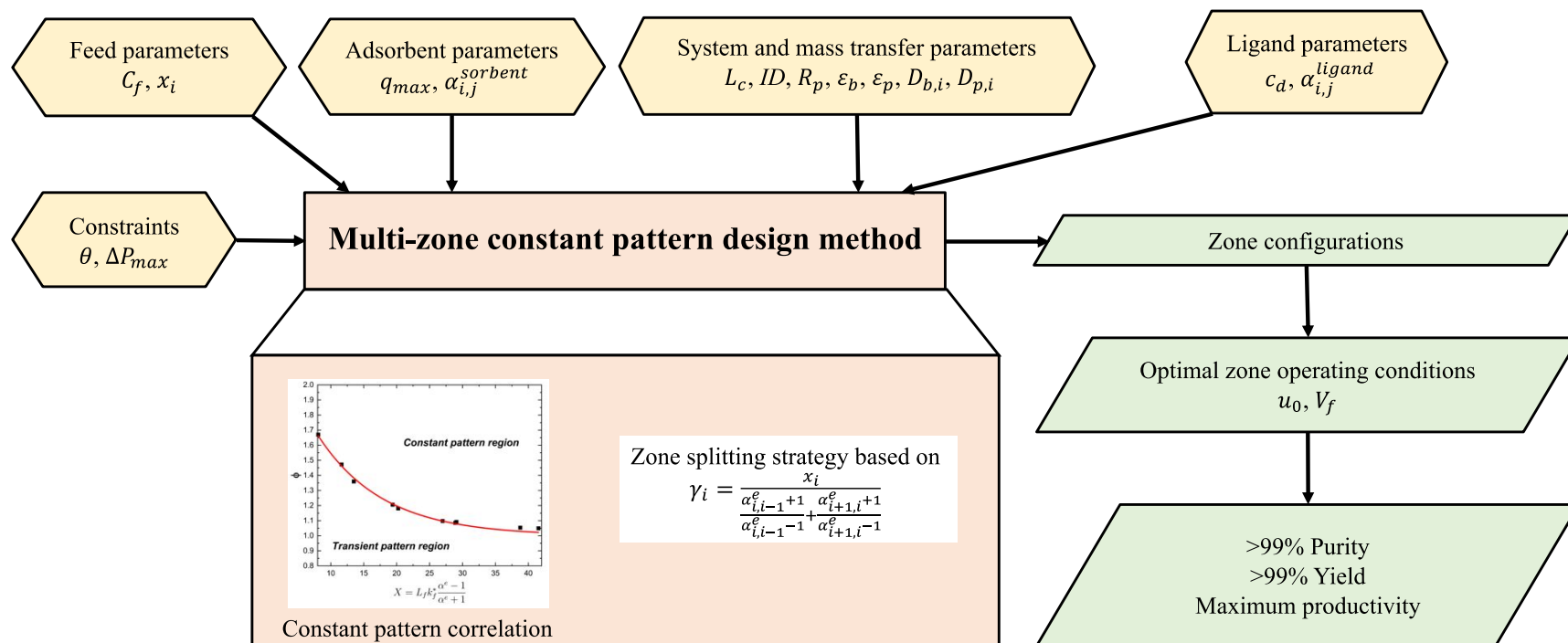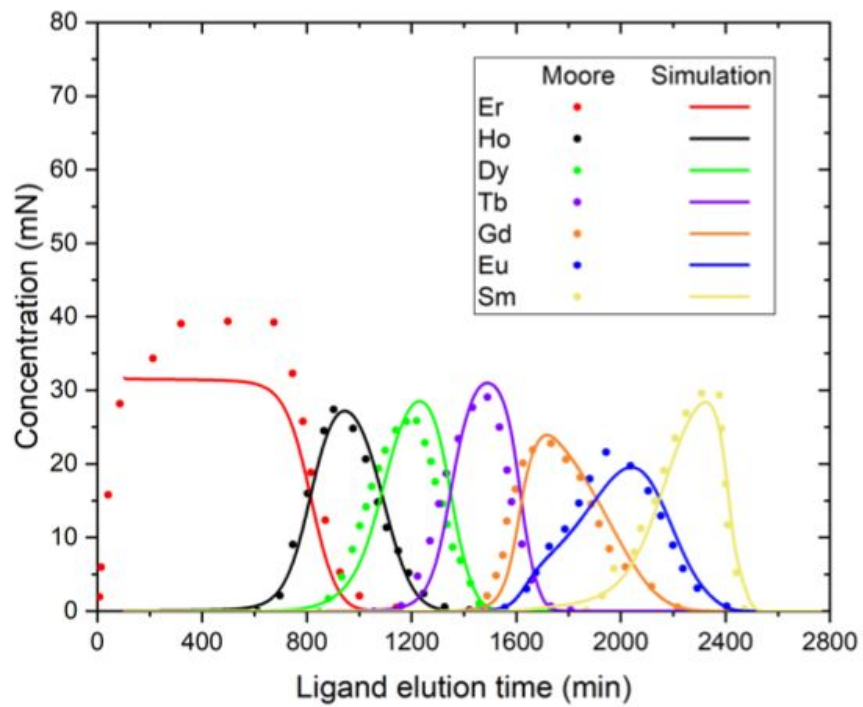
*Figure 7. Overview of the multi-zone constant pattern design method.*

*Figure 8. A schematic design of two-zone LAD for the separation of REE crude simulant derived from waste magnets. Zone I aims to recover high purity Nd. In Zone II, Column II-A aims to recover high purity Dy and Nd. Column II-B aims to recover high purity Nd and Pr.*

1

2

Figure 9. The experimental results from Moore et al. and the simulated chromatogram using the improved rate model simulations.

5

4
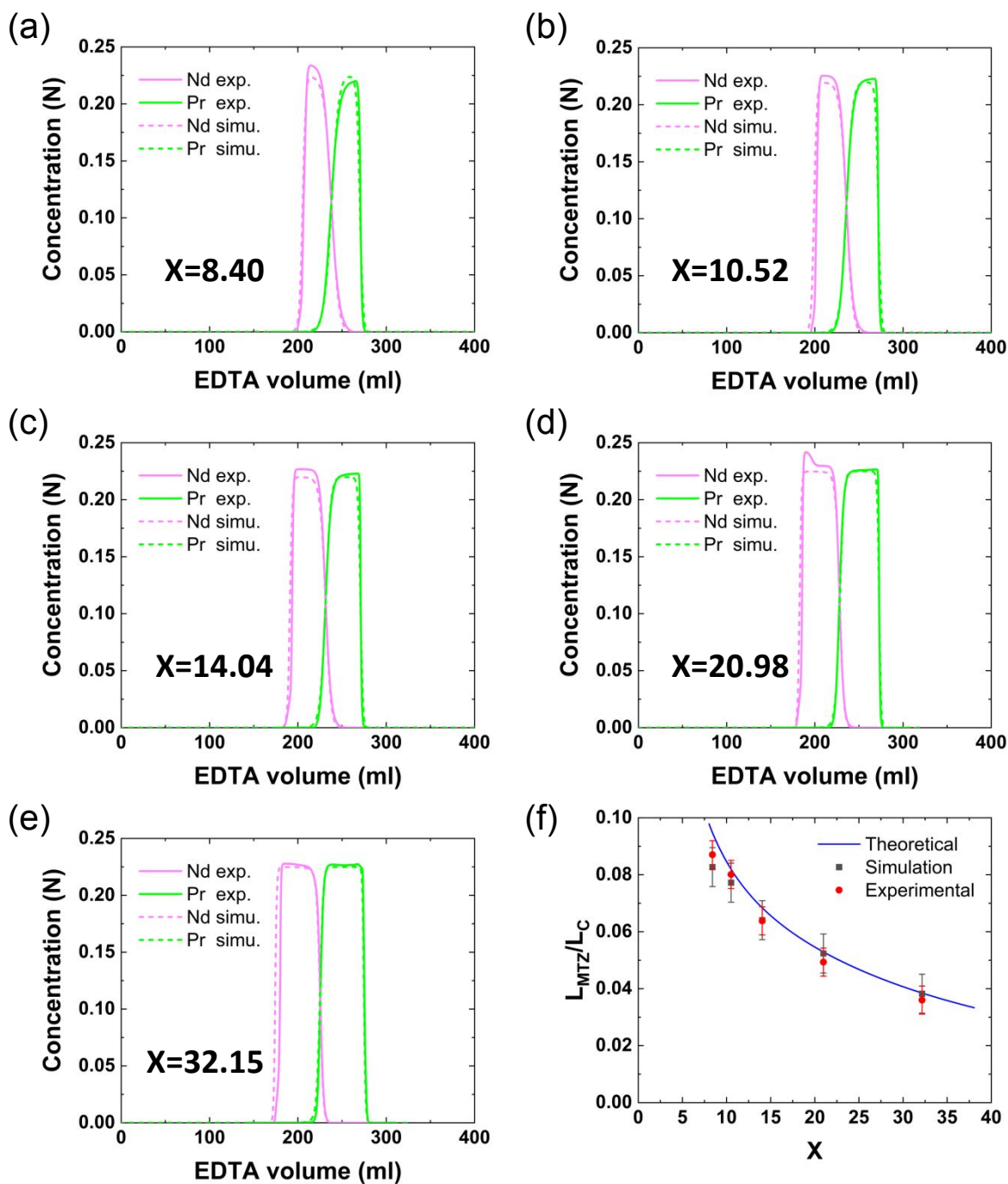
Figure 10. The separation of equimolar mixture of Nd and Pr (0.3 N) using 0.09 M EDTA-Na (pH 9). The experiments were designed for different X values: (a)8.40; (b)10.52; (c)14.04; (d) 20.98; (e)32.15. The mass transfer zone lengths in experiments and simulations are compared in (f). Simulation parameters and experimental conditions are listed in Supplementary Information Table S2.
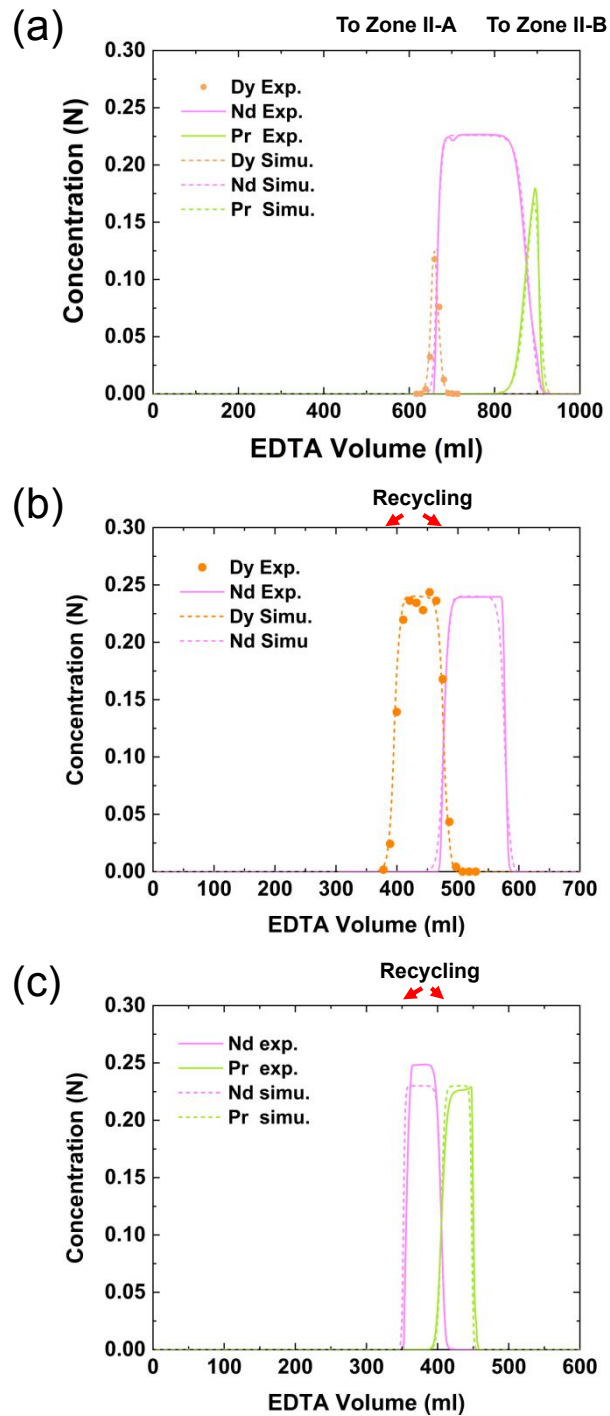
13

14   *Figure 11. Elution profiles of LAD tests for (a) Zone I: obtaining the majority of Nd. The two*

15   *mixed bands, Dy-Nd and Nd-Pr mixed bands (grey shade), were sent to Zone II for further*

16   *separation; (b) Zone II Column A: separating Dy and Nd from the mixed band generated in Zone*

17   *I; (c) Zone II Column B: separating Nd and Pr from the mixed band generated in Zone I. In both*

18   *Zone II Column A and B, the mixed bands (grey shade) will be recycled to their original feed*

19   *solution (mixed bands from Zone I).*

20